

Viscous Drag by Cellular Automata

J. A. M. S. Duarte^{1,2} and U. Brosa²

Received October 26, 1989

A simple method to compute the drag coefficient of two-dimensional bodies with arbitrary shapes is presented. The procedure is based on cellular automata as an extreme idealization of the molecular dynamics of a viscous fluid. We verify the algorithm by examples and obtain results in quantitative agreement with experiments even when eddies behind the obstacle are formed.

KEY WORDS: Hydrodynamics; multispin coding; molecular dynamics; vector computer.

1. INTRODUCTION

Lattice gas models have been the object of intense study since their definitive formulation by Frisch *et al.*⁽¹⁾ They showed that these discrete Boolean models with suitable rules of evolution imposed by conservation laws for the mass, momentum, and energy have associated dynamical laws which approximate the Navier–Stokes equations. In two dimensions this is achieved on the triangular lattice owing to the isotropy of the fourth-order tensors arising in the limiting process (see the Chapman–Enskog expansion⁽²⁾). Simulation of two-dimensional hydrodynamics by cellular automata (CA) is therefore so easy^(3–6) that it takes no more than 20 Fortran statements⁽⁷⁾ to program the salient steps.

When one compares this method with the application of finite elements⁽⁸⁾ or spectral methods,⁽⁹⁾ one must admit that cellular automata are inferior when accuracy within short computational time is required. However, the numerical stability of the CAs is unsurpassed. Also matchless is the ease with which even very complicated boundaries can be taken into account. These two properties make CAs a convenient tool for the com-

¹ Departamento de Física, Universidade do Porto, 4000 Porto, Portugal.

² HLRZ c/o KFA, Postfach 1913, D-5170 Jülich, Federal Republic of Germany.

putation of drag coefficients. This is a standard problem in hydrodynamics, which has been solved for many simple obstacles. Of interest, therefore, are complicated shapes. It is hard to build a complicated shape into a spectral code; it is easier with finite elements, but here general experience is that finite-element programs become unstable if a too involved geometry is set up.

The drag coefficient can be defined as

$$c_D := F/\frac{1}{2}\rho U_0^2 A \quad (1)$$

So if the body is inserted into homogeneous flow with density ρ and velocity U_0 , it exposes its cross-sectional area A to the stream. F is the force of resistance. Theoretically one may find it from the stress tensor, which contains the pressure and certain derivatives of the modified velocity field $\mathbf{v}(x, y, t)$. The pressure, in turn, is also obtained from the velocity field, namely via the Navier–Stokes equation. This, however, involves even double differentiations. CAs provide us with that velocity field, but with an accuracy so low that even single differentiations are problematic.

Naturally, we have a solution for this problem (Section 2). In Section 3 we describe our experience with this algorithm. We apply it then to the circular cylinder, to verify that decent numerical values come out, and treat another, more exotic case (Section 4). Due to restriction of computer memory, we had to exclude from our study turbulent flows, but we did computations in a range where long eddies are produced. We compare the computed eddies with those from experiments and find satisfactory agreement. This might be interesting because with the eddies the nonlinearity of the Navier–Stokes equation comes into play: We offer a quantitative confirmation of the CA method in the nonlinear regime (Section 5).

2. THE ALGORITHM

For the computation of the drag which acts on a body, it is useful to remember that CAs are nothing but idealized molecular systems bound to respect the elementary laws of conservation. And this, in particular the momentum balance, is all we need to find the resistance. Namely, F in (1) is just the force which the molecules exert on the body. From Newton we know

$$\frac{\Delta p}{\Delta t} = f \quad (2)$$

i.e., the momentum transfer Δp gives the force f which the body experiences from a single collision. We have only to look for all collisions of CA par-

ticles with the obstacle and to collect their velocity changes. This produces the desired F of (1), without any differentiation. Altogether we find

$$c_D = \frac{2 \sum_i \Delta v_i^{\parallel}}{U_0^2 \rho L (\Delta t / m)} \quad (3)$$

where summation has to go over all particles which hit the body at a given instant t . The v_i^{\parallel} are the velocity components of these particles parallel to the basic flow. Furthermore, we have ρL as a substitute of ρA in Eq. (1) as we are concerned with a 2D problem, so that c_D on the left-hand side of (3) denotes the drag coefficient per length unit. Δt and m are the time step and mass, respectively, both of which we choose to be unity.

Units must be handled with care. We use the distance between nearest neighbors in the triangular lattice as the length unit and one sweep through the lattice as the time unit. Furthermore, we embed a Cartesian coordinate system so that the bases of the triangles are parallel to the x axis. Lengths in the x direction are therefore given directly by the number of grid points l_x . But for lengths in the y direction, the points l_y must be multiplied by $\cos 60^\circ = \sqrt{3}/2$. Fortunately, ρL in (3) is an invariant under such transformations. ρL is simply equal to the number of grid points across the span, since we have, in the average, one particle per node. On the contrary, the factor $\sqrt{3}/2$ plays a role in the formula for the Reynolds number

$$\text{Re} = \frac{U_0 L / 2}{\nu} \quad (4)$$

The main example for such calculations is the cylinder. Therefore it is customary to compute Re with the radius of the body rather than with its total span L . We put the x axis parallel to the basic flow. Hence the span must be taken in the y direction. As we work with the collision rules of ref. 7, the effective viscosity ν is about 0.55. The velocity U_0 was chosen to be 0.21. This keeps unrealistic compressibility effects comfortably below the dangerous limit.⁽¹⁰⁾

To create a suitable environment for "measurements" of the drag, we set up a "square" lattice $l_x = l_y$ and force non-slip boundary conditions at $y_{\min} = 0$ and $y_{\max} = l_y \sqrt{3}/2$ by inversion of velocities.⁽³⁾ For these boundary conditions special collision tables are needed, which, however, are easily constructed by the rules given in ref. 7. In this oblique "channel" we install Poiseuille flow

$$\mathbf{v}(x, y, t = 0) = \frac{4U_0}{y_{\max}^2} y(y_{\max} - y) \mathbf{e}_x \quad (5)$$

by suitable Monte Carlo sampling of the initial velocities. \mathbf{e}_x is a unit vector. Flux conservation is guaranteed by periodicity.

Hence we have l_x Poiseuille profiles on the stack. We retain 200 of them. When the flow goes on, we insert these profiles at $x_{\min}=0$ and $x_{\max}=l_x$, selecting randomly one of the 200 profiles after each sweep, to maintain boundary conditions at the open ends. If one would stick to one profile, its fluctuations would propagate into the interior and distort the flow.

The obstacle is defined by two fields, YFRONT and YBACK, to describe the shape in the xy plane. Shapes with numerous bulges require several YFRONTS and YBACKS, but there is no problem in such an extension. Along these fields inversion of velocities is applied, just the same as used for upper and lower borders. What is now important is that one can work over YFRONT and YBACK *a posteriori*, that is, one sweeps through the grid as if there were no obstacle. After each sweep one replaces the velocities on the surface of the body. This avoids many IFs and therefore keeps a vector computer going.

A copy of the Fortran program is available from the authors. The main loops are published.⁽⁷⁾

3. INSERTION, RELAXATION, AND ALL THAT

Immediately after initialization we insert the body. The sudden insertion causes, of course, unphysical shocks, which, however, relax so that after some time the steady flow about the body emerges. Figure 1 illustrates such a relaxation. We see that after about 3000 time steps the giant fluctuations disappear, and just the normal ones, belonging to the stationary regime, remain. From our experience with lattices of different sizes $l_x \times l_y$ we derived

$$t_{\text{relax}} \approx l_x l_y / 1000 \quad (6)$$

as a rule of thumb. This expands computational times very much as soon as flows with somewhat higher Reynolds numbers are simulated. For example, our biggest grid was 2800×2800 , permitting us computations at $\text{Re} \approx 100$. In this case it took about 3 hr of CPU time on a single processor of a Cray-YMP to find a drag coefficient. This again underlines the necessity to construct CAs with viscosities as small as possible.⁽¹¹⁾

But even the equilibrium fluctuations are not small. Those shown in Fig. 1 are already averages over 50 time steps. To obtain good values for the drag coefficient c_D , we extend the computation until $2t_{\text{relax}}$ and average over all equilibrium steps.

Normally drag coefficients are given for homogeneous basic flow. We, in contrast, work with a Poiseuille stream as basic flow. However, all our

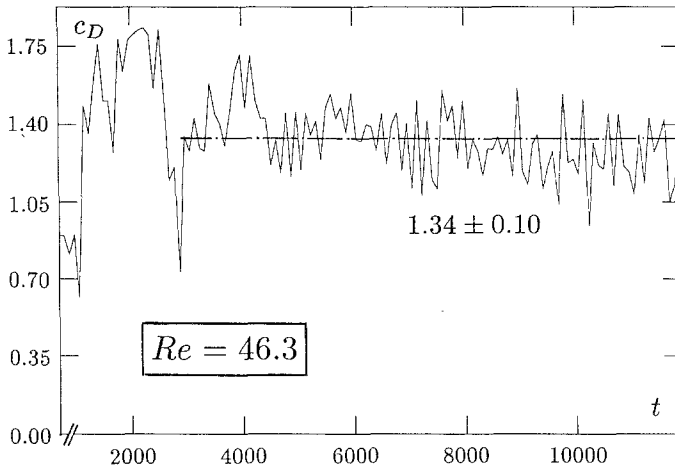


Fig. 1. The drag coefficient c_D of the hexagon as a function of time t . The computation was done on a 1600×1600 grid and the hexagon had a span of 280 grid points in the y direction. This corresponds, in accordance with (4), to the Reynolds number given in the figure. Also indicated is the long-time average of c_D used for Fig. 2. The fluctuations of c_D for the times $0 < t < 700$ not shown here are so big that they would dwarf everything else.

obstacles have a span that occupies less than 20% of the total channel width. Since we put the bodies on the centerline of the channel, we know that due to the parabolic profile (5) errors should be just a few percent. This is acceptable because the total accuracy of our method is not better than 10%. What is of concern is the x direction; the bodies are placed into the first third of the channel to make the wake visible.

4. DRAG AS A FUNCTION OF REYNOLDS NUMBER

We have applied the procedures described in the previous two sections to the cylinder and a hexagon. For the cylinder an analytic solution is known⁽¹²⁾

$$c_D = \frac{8\pi}{\text{Re}} \frac{1}{1 - 2 \log(\gamma \text{Re}/4)} \tag{7}$$

with $\gamma = 1.781072\dots$. Equation (7) holds only for very small Reynolds numbers, $\text{Re} < 1$. Nevertheless, it is useful if one wants to check the viscosity of a CA. Wieselsberger's measurements of the drag coefficient extend to $\text{Re} = 10^6$.⁽¹³⁾ Part of them are shown in Fig. 2 by the solid line. Our computed values, shown by the solid circles, agree within 10%. In addition, we have computed drag coefficients for the body displayed in Fig. 3. The

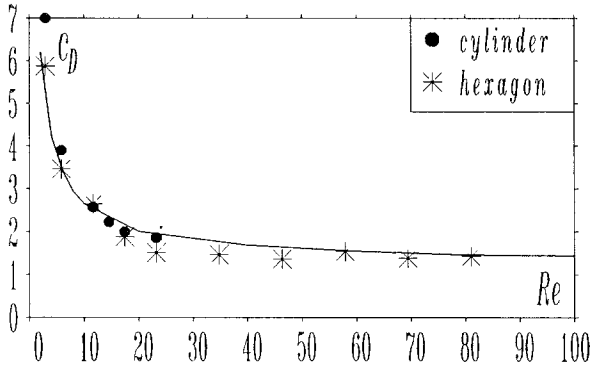


Fig. 2. Stationary values of the drag coefficient c_D as a function of Reynolds number Re .

results, indicated in Fig. 2 by the stars, exhibit the same general trend as those for the cylinder. However, they are systematically smaller at the smaller Reynolds numbers, probably due to the sharp rear edge.

5. FORMATION OF EDDIES BEHIND A BODY

Equation (7) becomes hopelessly wrong as soon as the slightest wake is formed. Our method, however, performs well even if long eddies are

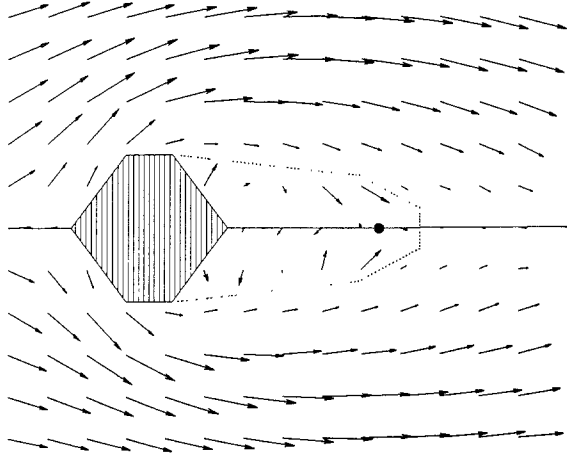


Fig. 3. Stationary flow past the hexagon at $Re = 23.1$. The straight centerline was drawn only for orientation. Inside the area distinguished by the dotted line, the velocity vectors were magnified by the factor 5. This is because in the region of recirculation velocities generally are quite slow. The turning point is marked by the blob. One may note that the velocities on the centerline before and behind that blob have opposite x directions. Thus, one can measure the length of the eddies and check if the value given in Fig. 4 is right. This picture was obtained by superposition of stationary velocity fields on eight different lattices⁽⁷⁾ at eight different times.

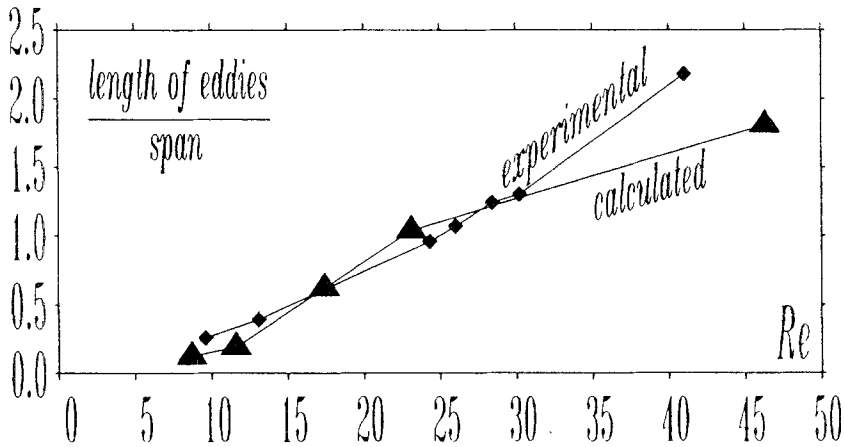


Fig. 4. Dimensionless length of eddies behind the hexagon as a function of Reynolds number Re . The drawn lines are just to guide the eye.

generated. An example is shown in Fig. 3. The turning point, where the back flow ends, can be remarkably well identified. One even recognizes the structure of the eddies, even though this is at the limits of accuracy of the present method.

The computed positions of the turning points can be compared with experimental values (see Fig. 4). One measures the distance between the rear edge of the body and the turning point and divides it by the span of the obstacle. Of course, experimentally only values for the cylinder are available.⁽¹⁴⁾ We spent most of our computational time for the hexagon, considering it as the more exotic object. Nevertheless, the agreement is as good as can be expected.

ACKNOWLEDGMENT

We thank D. Stauffer for his interest and support.

REFERENCES

1. U. Frisch, B. Hasslacher, and Y. Pomeau, *Phys. Rev. Lett.* **56**:1505 (1986).
2. S. Wolfram, ed., *Theory and Applications of Cellular Automata* (World Scientific, Singapore, 1986).
3. D. d'Humieres and P. Lallemand, *Complex Systems* **1**:599 (1987).
4. H. A. Lim, *Phys. Rev. A* **40**:968 (1989).
5. H. A. Lim, *Complex Systems* **2**:45 (1988).
6. F. Hayot, M. Mandal, and P. Sadayappan, *J. Comp. Phys.* **80**:277 (1989).
7. U. Brosa and D. Stauffer, *J. Stat. Phys.* **57**:399 (1989).

8. O. C. Zienkiewicz, *The Finite Element Method* (McGraw-Hill, London, 1977).
9. C. Canuto, M. Y. Hussaini, A. Quarteroni, and T. A. Zang, *Spectral Methods in Fluid Dynamics* (Springer, Berlin, 1988).
10. J. P. Dahlburg, D. Montgomery, and G. D. Doolen, *Phys. Rev. A* **36**:2471 (1987).
11. B. Dubrulle, U. Frisch, M. Hénon, and J.-P. Rivet, Low viscosity lattice gases, *J. Stat. Phys.*, to appear.
12. H. Lamb, *Hydrodynamics* (Cambridge University Press, Cambridge, 1975).
13. H. Schlichting, *Grenzschicht-Theorie* (Braun-Verlag, Karlsruhe, 1982).
14. M. Van Dyke, *An Album of Fluid Motion* (Parabolic Press, Stanford, California, 1982).

Communicated by D. Stauffer